

## THE USE OF WIDE BANDWIDTH HEAT TRANSFER GAUGES TO DIAGNOSE UNSTEADY TURBOMACHINERY FLOWS

M. L. G. Oldfield and R. W. Ainsworth  
University of Oxford

### ABSTRACT

This paper reviews the use of surface thin-film resistance thermometers as heat transfer gauges to detect and measure such unsteady phenomena as boundary layer transition, unsteady separations, wake and shock wave passing on turbine blades, either in cascades or fully rotating experiments. Different types of gauges (semi-infinite on MACOR, layered and Kapton stuck-on) are discussed, along with the problems and limitations encountered in using them to study unsteady flows. The use of electrical analogue circuits to pre-process the thin film gauge signal is discussed, along with bandwidth and time-delay measurements of practical circuits.

### NOMENCLATURE

$a_1$	substrate thickness	$w$	gauge width
$c$	thermal capacity	$v$	velocity
$f$	frequency	$v_f$	change in gauge voltage
$k$	thermal conductivity	$V_O$	output voltage
$I$	film current	$\rho$	density
$M_{exit}$	exit Mach number	$\sqrt{(\rho c k)}$	thermal product
$\dot{q}$	heat transfer rate	$\tau$	rise time
$R_f$	gauge resistance	$\omega$	angular frequency
$t$	time		
$T_g$	gas temperature		
$T_s$	surface temperature		

### 1. INTRODUCTION

The use of thin film thermometers to measure steady and unsteady heat transfer rates to the surface of turbine blades, re-entry bodies and other test models immersed in aerodynamic flows is well established [1,2,3]. To those working with these gauges it has become apparent that the interpretation of these signals can yield much useful information of gas flows and boundary layers. This paper reviews the aerodynamic interpretation of such signals, and the associated electronic and computer data processing needed.

Of course, conventional hot wire and hot film probes (manufactured by DANTEC, TSI and others) also depend on the measurement of unsteady heat transfer. These are well known and documented [4] and will not be dealt with here. This paper deals with the aerodynamic information which can be gleaned from thin film gauges mounted on the surface of relatively large bodies immersed in the flow.

## 2. THE BASIC TECHNIQUE

Fig. 1 illustrates the basic concept of the technique. The array of thin film gauges is mounted on a body at surface temperature  $T_s$  in a gas flow at a different total temperature  $T_g$ . The driving temperature ( $T_g - T_s$ ), created by heating or cooling either the surface or the gas, is essential in order to drive a heat transfer rate  $\dot{q}$  to the surface. Fluctuations in  $\dot{q}$  due to flow features cause small fluctuations in  $T_s$ , and hence in the film gauge resistance  $R_f$ . The fluctuations in  $R_f$  are electronically processed into a voltage signal proportional to  $\dot{q}$  and this is used to infer aerodynamic conditions in the flow and boundary layer.

**Advantages** of the technique are:

- \* Non intrusive;
- \* Wide bandwidth (0 - 100 kHz);
- \* Multi-channel;
- \* High sensitivity ;

**Disadvantages** include:

- \* Measurements are taken on the surface only ;
- \* Gauges are difficult to make;
- \* A temperature difference ( $T_g - T_s$ ) is needed;
- \* The electronics are expensive.

## 3. DETECTABLE FLOW FEATURES

Fig. 2 lists some of the flow features which can be studied using thin film gauges, along with their characteristic frequencies. They include:

- \* Boundary layer **transition**, where turbulent spots transiently lift  $\dot{q}$  from low laminar to high turbulent levels at 200 Hz - 10 kHz;

\*Unsteady boundary layer **separation** characterised by dips in  $\dot{q}$  at low ( < 1 kHz ) frequency;

\***Wake passing**, typically on a turbine blade cutting the wakes of a preceding nozzle guide vane (NGV) blade row. The highly turbulent wakes cause short bursts of high heat transfer at the blade passing frequency ( ~ 5 kHz);

\***Shock wave passing**, e.g. from the trailing edges of an upstream blade row. As shock waves and associated expansions pass over a gauge the rapid compression or expansion of the boundary layer gives rise to rapid large excursions in  $\dot{q}$  .

The turbulence in a fully developed turbomachinery boundary layer has a characteristic frequency given by

$$f \sim \frac{\text{velocity}}{\text{thickness}} \sim \frac{300 \text{ m/s}}{1 \text{ mm}} \sim 300 \text{ kHz}$$

This is too high to be seen by thin film gauges. Consequently, it may be difficult to distinguish between a laminar and a fully turbulent boundary layer if there are no measurements in the intervening transition region.

#### 4. THIN FILM GAUGES IN USE

Owen [5] used thin films on a flat plate with constant temperature hot-wire anemometers to study transition. As can be seen from the traces of the a.c. film signal in Fig. 3, turbulent spot generation is associated with large fluctuations in heat transfer. In the turbulent flow region, the rms level drops as the characteristic frequencies of the fluctuations rise beyond that detectable by the instrumentation.

The use of this technique on a turbine blade in the large cascade at DFVLR Braunschweig was reported at the 1979 Leatherhead meeting of this Symposium [6,7].

Transition can be seen even more clearly if the absolute heat transfer rate is measured, as well as the fluctuating a.c. component. Fig. 4 shows fast heat transfer traces taken by thin film gauges on the suction surface of a gas turbine blade, from [8,9]. The transition induced by 2% freestream turbulence is clearly seen by comparison with the laminar heat transfer rate.

In an experiment which simulated the passing of upstream nozzle guide vane shock waves and wakes over a moving rotor blade, the unsteady heat transfer rate signals shown in Fig. 5, from [10], clearly show a spike due to the shock wave followed by a pulse of enhanced heat transfer excited by the wake. Interestingly, in this case, the shock "spike" was shown to be due to a collapsed, moving, separation bubble generated as the shock wave passed the blade leading edge, and not to the direct shock impingement on the surface.

In a similar experiment on a transonic turbine blade profile [11] stronger NGV trailing edge shock waves ( $M_{exit} = 1.13$ ) were simulated, and the unsteady pressure signals were measured by small, wide bandwidth pressure transducers placed at the same locations as the thin film gauges. In this case, Fig. 6(b), the shock waves underwent multiple reflections in the turbine passage, causing large transient pressure fluctuations. There were large associated heat transfer transients (Fig. 6(a)), and it was shown that a simple model could predict these fluctuations from the shock induced pressure fluctuations. It can be seen that the surface thin film gauge is a good detector of passing shock waves.

## 5. TYPES OF THIN FILM GAUGES

As can be seen in Fig. 7, surface thin film gauges fall into two general categories. Firstly, they can be mounted on a substrate which is considered semi-infinite [1], where, for example, a thin film platinum resistance thermometer is fired onto a MACOR, quartz or glass substrate. Secondly, there are layered gauges where, for example, a thin insulating layer such as vitreous enamel [12], or Kapton [13], covers a substrate, usually metal, having different thermal properties. This second type includes systems where the gauges are evaporated onto a plastic film which is then adhesively bonded to the model. In practice, this alters the low frequency characteristics of the gauge only. At high frequencies most gauges can be considered to be semi-infinite. It can be shown [14] that gauges are semi-infinite for times less than

$$t = \frac{\pi}{4} \left( \frac{a_1}{k_1} \right)^2 \frac{(\rho_1 c_1 k_1)}{(\rho_2 c_2 k_2)} \left( \sqrt{(\rho_1 c_1 k_1)} + \sqrt{(\rho_2 c_2 k_2)} \right) \quad (1)$$

Unfortunately, equation (27) of [14] contains a transcription error and should read as (1) above.

For a typical layered thin film gauge with a 75  $\mu\text{m}$  thick Kapton layer ( $\sqrt{(\rho_1 c_1 k_1)} = 490 \text{ J m}^{-1} \text{ s}^{-1/2} \text{ K}^{-1}$ ,  $k = 0.155 \text{ W m}^{-1} \text{ K}^{-1}$ ) on a Nickel substrate ( $\sqrt{(\rho_2 c_2 k_2)} = 18,300 \text{ J m}^{-1} \text{ s}^{-1/2} \text{ K}^{-1}$ ), the gauge acts in a

semi-infinite manner for 47 ms, a time much longer than those typical of transition or wake passing signals.

## 6. PHYSICAL LIMITATIONS OF THIN FILM GAUGES

The physical size of the thin film gauge restricts the maximum frequency response in three ways (Fig.8):

The **thickness** of the film must be small in order for it to respond at high frequencies [1]. For a 100 kHz response, the gauge thickness must be less than about 0.5  $\mu\text{m}$ .

The **width**  $w$  of the film and the flow velocity  $v$  limit the rise time to a minimum of  $\tau = w/v$ . For example, a 100 kHz bandwidth requires  $\tau < 1.6 \mu\text{s}$ ; with a flow velocity of 300 m/s, this would give a maximum film width  $w < 0.5 \text{ mm}$ .

The **length** of the film is important when three dimensional disturbances, such as turbulent spots, are to be detected. The gauge integrates the heat transfer over its length (Fig.8), and the signal will not rise to the full value if the spot, say, does not cover the active length of the gauge.

It obviously pays to keep the gauges as physically small as possible.

## 7. FREQUENCY RESPONSE OF SEMI-INFINITE GAUGE

A one dimensional, unsteady, heat-transfer analysis of the semi-infinite thin film heat transfer gauge shows that, in the frequency domain, the surface (or gauge), temperature  $T_s$  is related to the surface heat transfer rate  $\dot{q}$  by the expression

$$T_s = \frac{1}{\sqrt{(j\omega)}} \frac{1}{\sqrt{(\rho ck)}} \dot{q} \quad (2).$$

This is plotted in Fig. 9. There is a wide variation of sensitivity with frequency, e.g. a factor of  $10^3$  over the range 0.1 Hz to 100 kHz. This gives rise to problems if the  $T_s$  signal is directly digitised: e.g. on a 10 bit A/D, a  $\dot{q}$  signal corresponding to full scale at 0.1 Hz would give only a one bit change at 100 kHz ! It is, therefore, important to electrically process the continuous thin film signal before digitising it, and the amplifiers used should have greater gain at higher frequencies, preferably approximating to a  $\sqrt{(j\omega)}$  characteristic.

We shall now look at the two main methods of electrically processing the signal.

## 8. CONSTANT TEMPERATURE OPERATION

In the constant temperature mode of operation, the thin film gauge forms one arm of a Wheatstone bridge (Fig. 10) and feedback is used to keep the gauge resistance  $R$ , and hence  $T_s$  constant. The amplifier output voltage  $V_O$  is used to measure the electrical heating power to the gauge,

$$\text{Power} \sim V_O^2 \sim \dot{q}_{flow} + \dot{q}_{substrate} \quad (3)$$

This is, of course, the same system as used with constant temperature hot wire anemometers.

### Advantages:

It is commonly used in continuously running tunnels, as it has the convenience of heating the thin film directly to provide the necessary  $(T_g - T_s)$ , negative in this case. The negative feedback keeps the frequency response flat to  $\sim 20$  kHz and also prevents the film from accidentally overheating.

### Disadvantages:

The electronics are expensive, especially for multi-channel systems and the bandwidth is limited by stability considerations. As  $\dot{q}_{substrate}$  usually exceeds  $\dot{q}_{flow}$ , the constant temperature mode is better for measuring fluctuating  $\dot{q}$  than for determining mean heat transfer levels.

## 8. CONSTANT CURRENT OPERATION

In the constant current mode of operation, a small, constant sensing current  $I$  is passed through the thin-film gauge in order to generate a change of voltage proportional to the change of film resistance with temperature. There is generally no attempt to heat the film with this current; usually care is taken to avoid this heating.

Fig. 11 shows a typical constant current circuit as used for heat transfer measurement [2,3]. The thin film voltage is passed through a lumped resistance-capacitance transmission line (or "**Analogue**"), which models the one dimensional, unsteady heat conduction in the substrate. The current through the analogue is proportional to the heat transfer rate to the film, and this is amplified to give an output voltage.

Constant current systems are commonly used in short duration wind tunnels, where the  $(T_g - T_s)$  required to drive  $\dot{q}$  is generated by either having a hot or cooled flow over a model at ambient temperature, or by preheating (or precooling) the model before the tunnel is run. The short duration avoids the cost of providing continuous heating or cooling power.

**Advantages:**

It measures both the time-mean and fluctuating components of heat transfer rates. Wide bandwidths ( 0.1 Hz - 100kHz) are possible, and the electronics are cheaper than with constant temperature systems. Low noise systems having a wide dynamic range are practicable.

**Disadvantages:**

It requires a temperature difference to operate, and the electronics are specialised.

A practical analogue circuit, from [3], for use with constant current thin film heat transfer gauges is shown in Fig. 12. The values of the resistors and capacitors in the R-C transmission line increase logarithmically such that only 9 sections are required to give the required  $\sqrt{(j\omega)}$  rising frequency characteristic from 0.023 Hz to 85 kHz. The current source and the current to voltage converter are optimised for low noise over this bandwidth. Many of these circuits have been used to take multichannel heat transfer measurements in turbine research facilities at Oxford and elsewhere.

Recently, concern has been expressed by others at the possibility of phase errors at high frequencies in these analogues leading to distortions in the shape of rapidly fluctuating heat transfer traces. Measurements of the frequency response of the circuit in fig. 12 , taken in collaboration with J.E. LaGraff, are shown in figs. 13 - 15.

Fig. 13 shows that the gain rolls off with a -3 dB limit of 85 kHz, with the rapid attenuation above this being mainly due to the low pass filter in the circuit. This filter is there to reduce high frequency circuit noise and interference. Fig. 14 shows that, indeed, there is considerable phase lag from the ideal  $45^\circ$  lead above about 3 kHz, and this could cause problems.

However when this phase lag is converted into a relative time delay plot, it can be seen that the delay time is, as was intended, constant at near  $4 \mu\text{s}$  right up to 100 kHz. This constant delay will result in only a small,  $4 \mu\text{s}$ , time shift in the measured signal, and there will be little distortion in the heat transfer rate waveforms measured, apart from attenuation of frequencies above 85 kHz.



## 9. A SUGGESTION FOR CONSTANT CURRENT SYSTEMS IN CONTINUOUS TUNNELS

A possibility worth considering with continuous wind tunnels is that of generating  $(T_g - T_s)$  by heating the thin film gauges with a greatly increased sensing current  $I$  in Fig. 11. Apart from the obvious **advantages** of saving on heating systems, there is also that of increased sensitivity, since the change in thin film voltage .

$$v_f \sim I R_f \sim \frac{q}{\sqrt{(\rho c k)}}$$

### Advantages:

Good sensitivity, wide bandwidth and cheaper electronics.

### Disadvantages:

It is more difficult to adjust  $(T_g - T_s)$ , and  $I$  may have to be turned off before stopping the tunnel flow in order to avoid burning out the film!

## 11. CONCLUSIONS

The wide-bandwidth, thin film, heat transfer gauge is an effective diagnostic tool for the experimental study of unsteady turbomachinery flows. It is rugged, non-intrusive and can be applied to the surface of test blades and other components in either continuous or short duration test facilities. The signal from thin films must be pre-processed before digitisation, and there are a number of established electronic systems to do this. It is to be hoped that the use of these gauges for aerodynamic work will become more widespread as the realisation of their strengths becomes more widely realised.

## 12. REFERENCES

1. Schultz, D.L. and Jones, T.V., 1973, "Heat Transfer Measurements in Short-Duration Hypersonic Facilities", NATO Advisory Group for Aeronautical Research and Development AGARDOGRAPH 165.
2. Oldfield, M.L.G., Jones, T.V. and Schultz, D.L., 1978, "On-Line Computer for Transient Turbine Cascade Instrumentation, IEEE Trans. AES, 14, pp 738.
3. Oldfield, M.L.G., Burd, H.J., and Doe, N.G., 1982, "Design of Wide-Bandwidth Analogue Circuits for Heat Transfer Instrumentation in Transient Tunnels", 16th Symp. of ICHMT, Dubrovnik, Hemisphere Publ.



4. **Comte-Bellot, G., 1976, "Hot Wire Anemometry", Annual Review of Fluid Mechanics, Vol. 8, pp 209-231.**
5. **Owen, F.K., 1970, "Transient Experiments on a Flat Plate at Subsonic and Supersonic Speeds", AIAA Journal, Vol. 8, No. 3, pp 518-523.**
6. **Oldfield, M.L.G. and Klock, R., 1979, "The detection of Boundary Layer Transition on a Gas Turbine Blade by means of Pitot Probe and Thin Film Technique", Proc. Symp. Measuring Techniques in Transonic and Supersonic Cascade Flow, C.E.R.L., Leatherhead.**
7. **Oldfield, M.L.G., Klock, R., Holmes, A.T. and Graham, G.C., 1981, "Boundary Layer Studies on Highly Loaded Cascades using Heated Thin Films and Traversing Probe", ASME, J. Eng. for Power, Vol. 103, pp. 237.**
8. **Doorly, D.J. and Oldfield, M.L.G., 1985, "Simulation of Wake Passing in a Stationary Turbine Rotor Cascade", J. Prop. and Power, Vol. 1, No. 4, pp 316.**
9. **Doorly, D.J., Oldfield, M.L.G. and Scrivener, C.T.J., 1985, "Wake Passing in a Turbine Rotor Cascade", AGARD CP 390.**
10. **Doorly, D.J. and Oldfield, M.L.G., 1985, "Simulation of the Effects of Shock Wave Passing on a Turbine Rotor Blade", ASME J. Eng. for Gas Turbines and Power, Vol. 107, No. 4.**
11. **Johnson, A.B., Rigby, M.J., Oldfield, M.L.G., Ainsworth, R.W. and Oliver, M.J., 1988, "Surface Heat Transfer Rate Fluctuations on a Turbine Rotor Blade due to Upstream Shock Wave Passing", ASME 33rd Int. Gas Turbine Conference., Amsterdam.**
12. **Doorly, J.E., and Oldfield, M.L.G., 1986, "New Heat Transfer Gauges for use on Multi-layered Substrates, ASME J. Turbomachinery, Vol. 108, No. 1, July 1986.**
13. **Epstein, A.H., Guenette, G.R., Norton, R.J.G., and Cao Yuzhang, 1985, "High Frequency Response Heat Flux Gauges for Metal Blading", AGARD-CP-390, Norway.**
14. **Doorly, J.E., and Oldfield, M.L.G., 1987, "The Theory of Multi-layer Thin Film Heat Transfer Gauges", Int. J. Heat Mass Transfer, Vol. 30, No. 6, pp.1159-1168, 1987.**

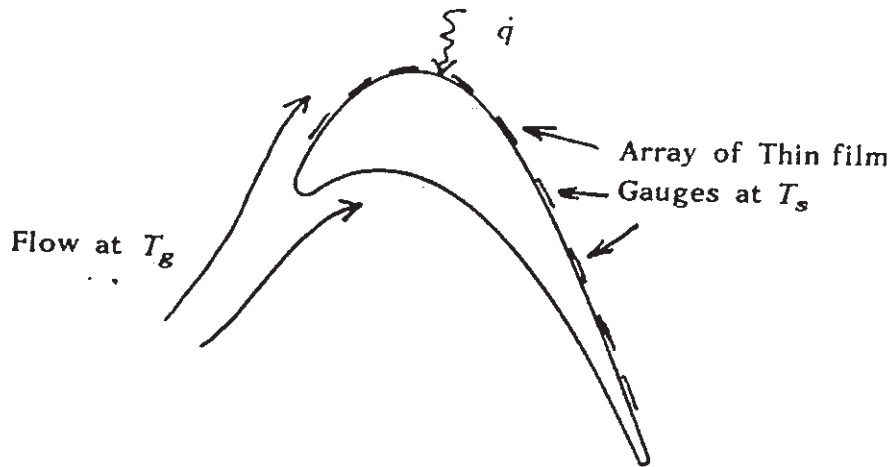


Fig. 1 Array of thin film heat transfer gauges mounted on a blade and used to measure unsteady flows.

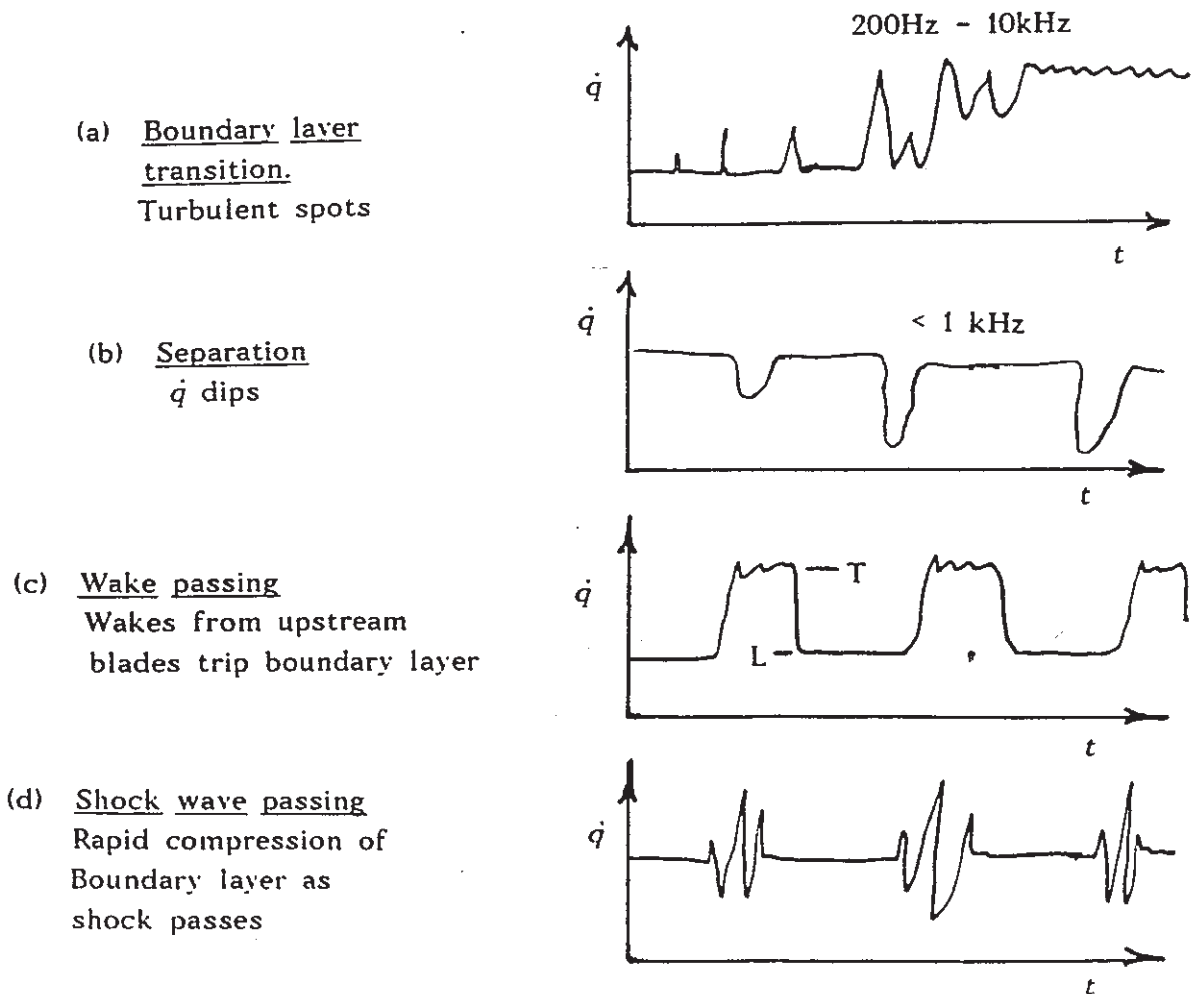


Fig. 2 Flow features which can be studied using thin film gauges.

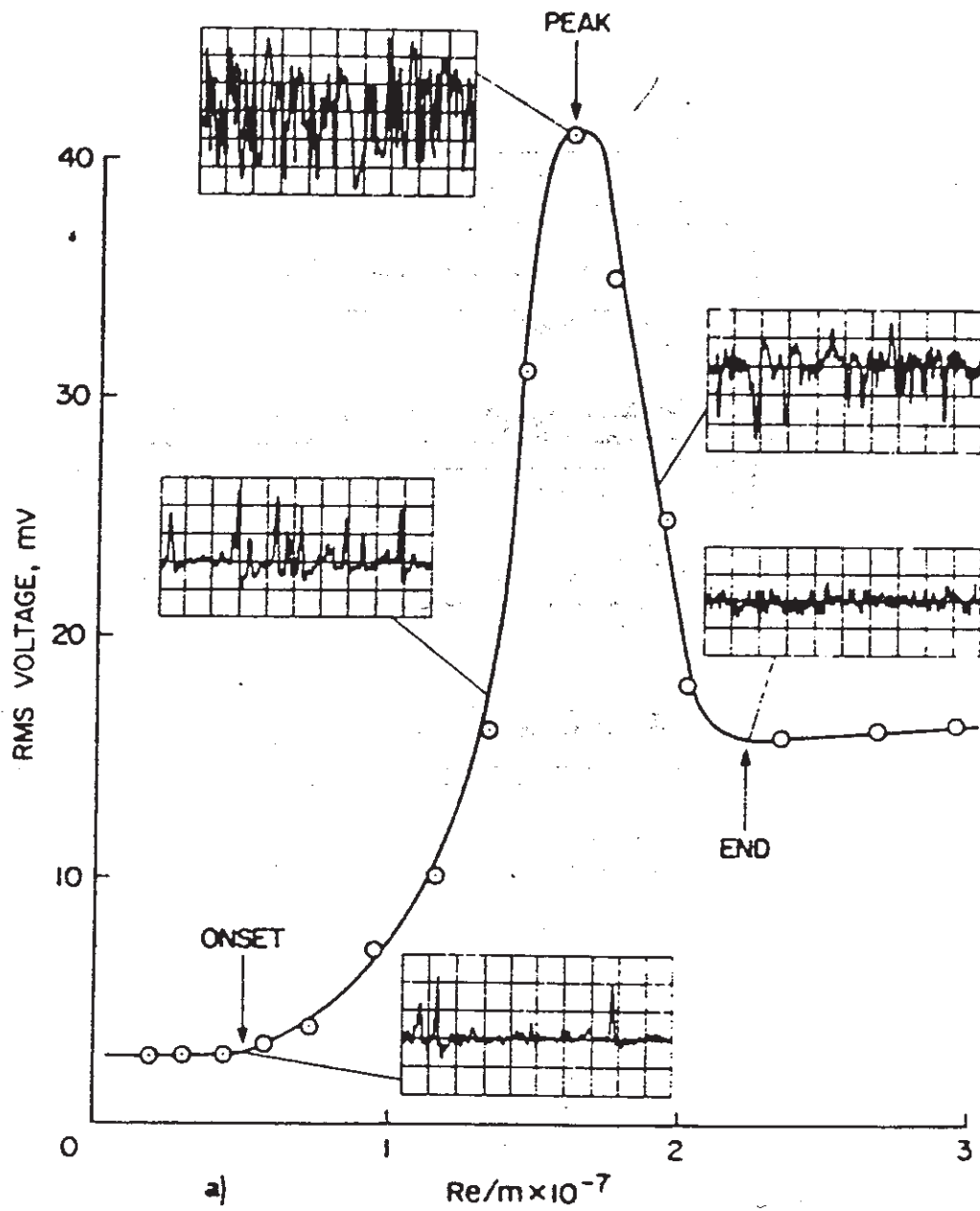


Fig. 3 Heat transfer fluctuations through transition region, as measured by Owen [5].

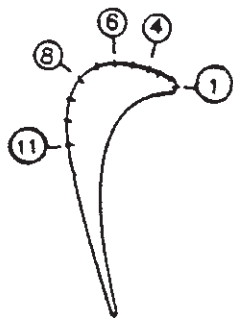
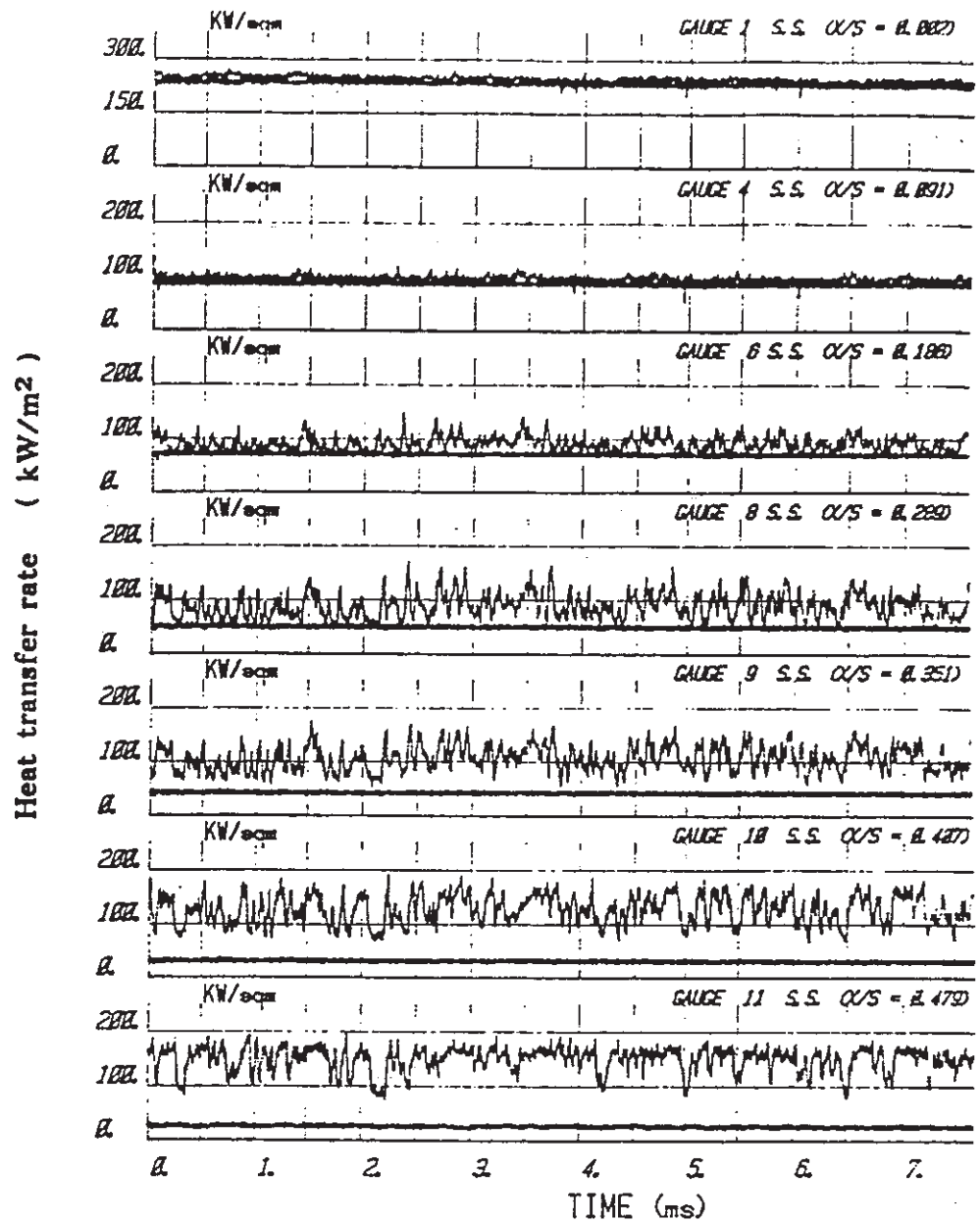


Fig. 4 Transition on a turbine blade suction surface with 2% free stream turbulence, as shown by wide bandwidth thin film gauges. the lower lines are laminar traces with < 0.4% turbulence. from [9].

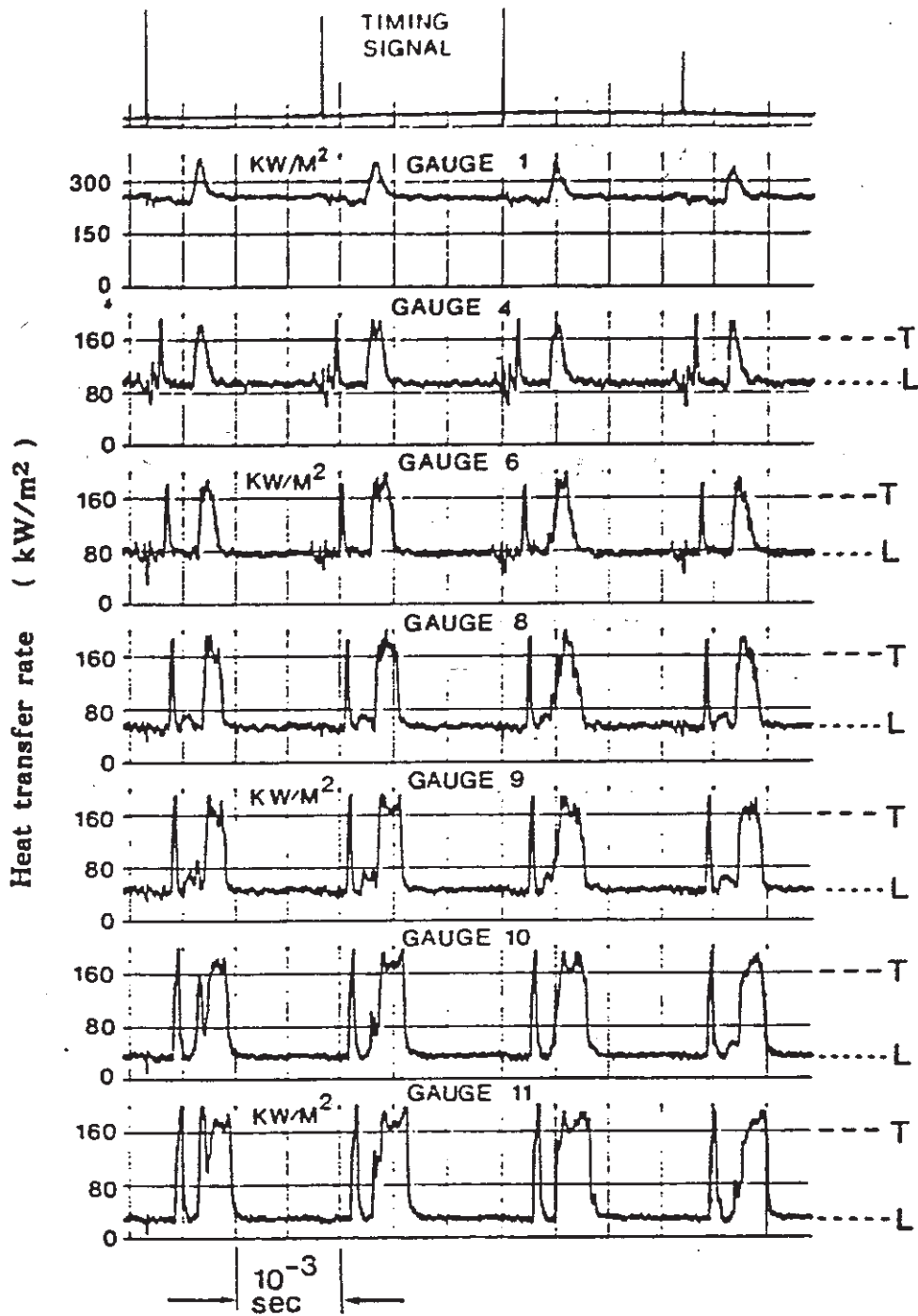


Fig. 5 The effects of isolated shock-wave and wake passing on the heat transfer to a blade suction surface. L and T refer to laminar and turbulent levels, respectively. From [10].

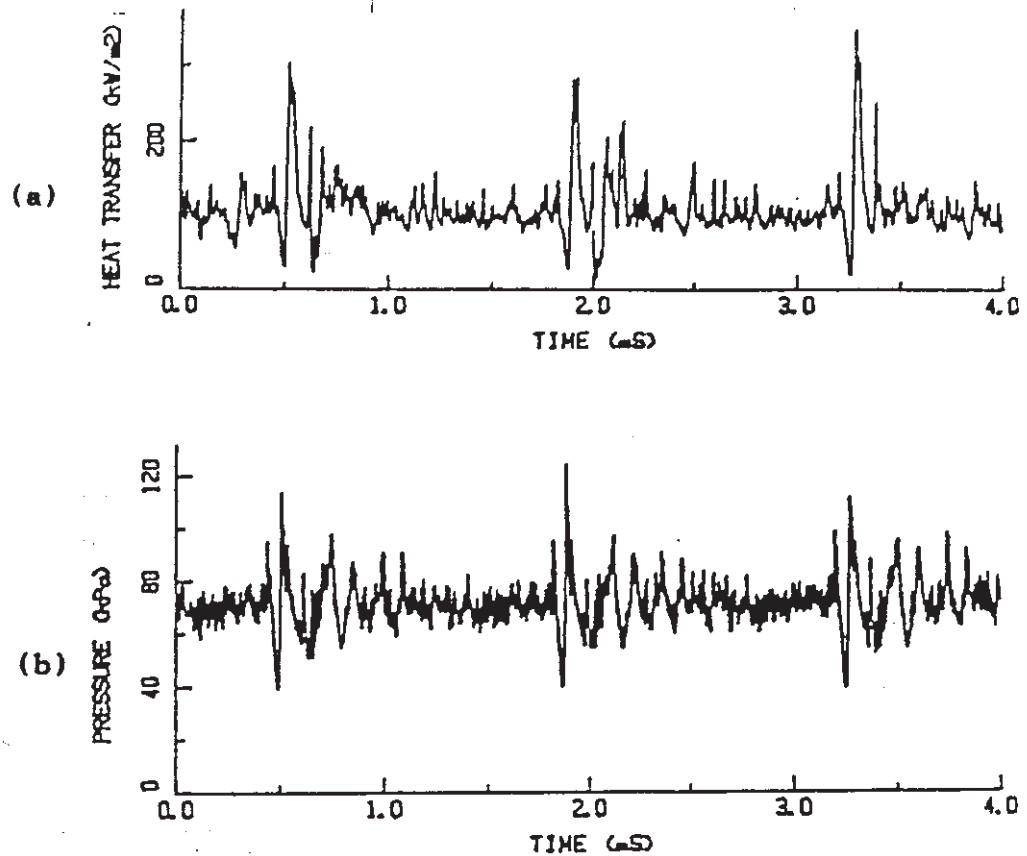


Fig. 6 Heat transfer rate fluctuations (a), and surface pressure fluctuations (b) due to the passing of strong shockwaves on a transonic turbine blade suction surface, from [11].

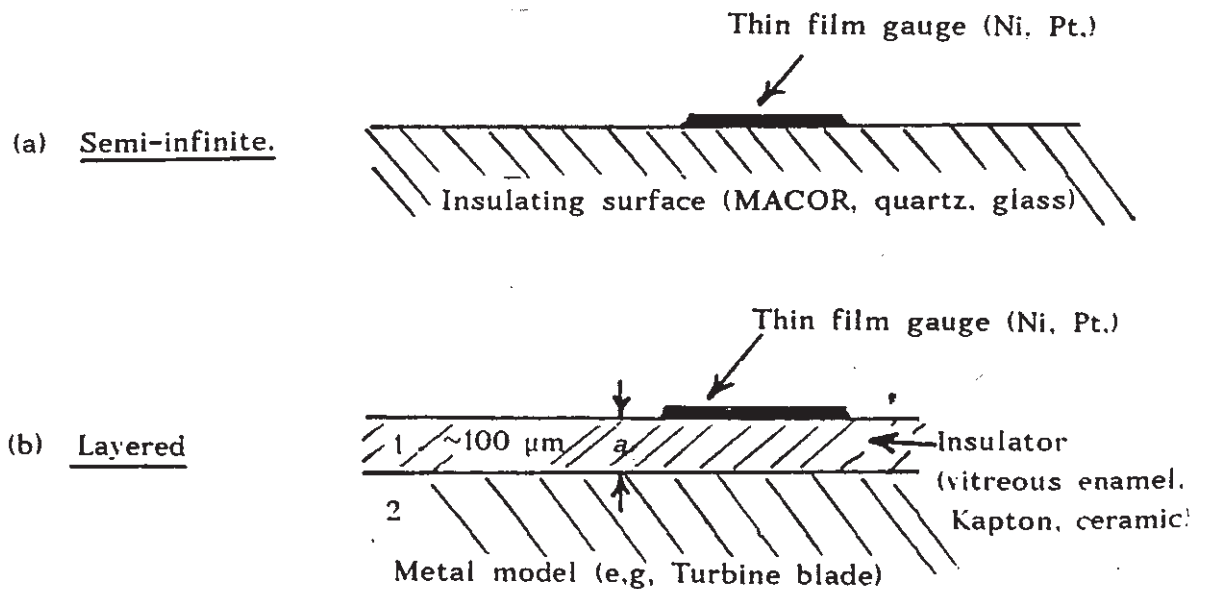


Fig. 7 Types of thin film gauges.

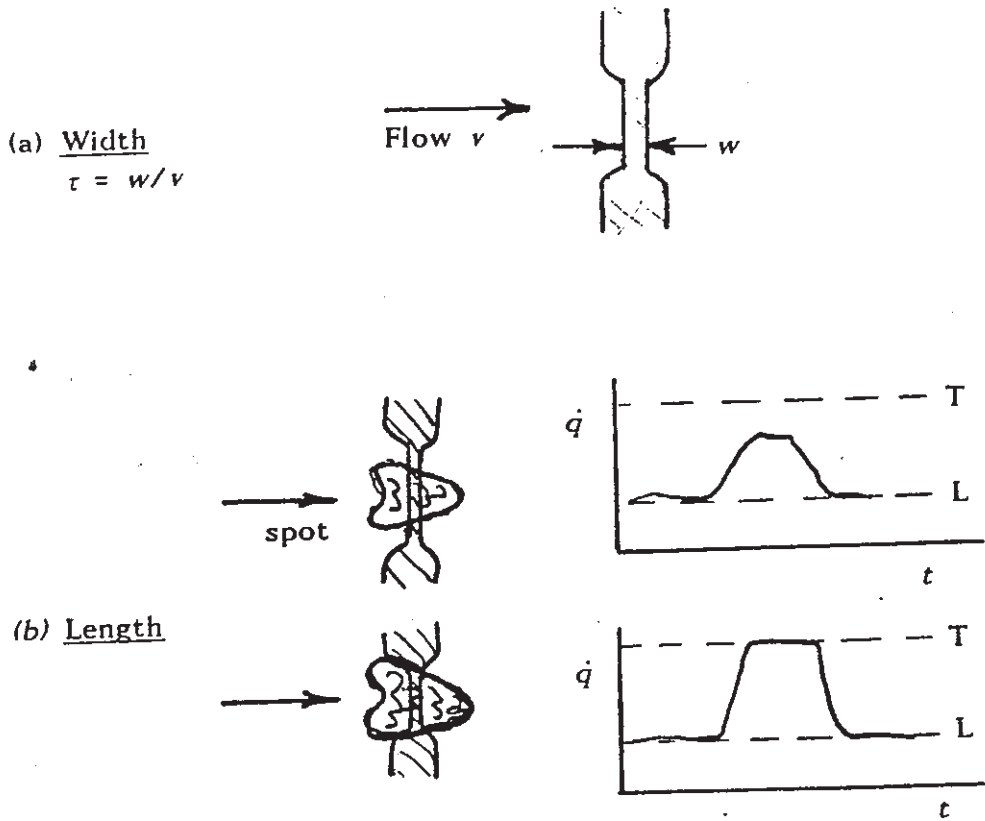


Fig. 8 The effects of width and length on thin film gauge frequency response.

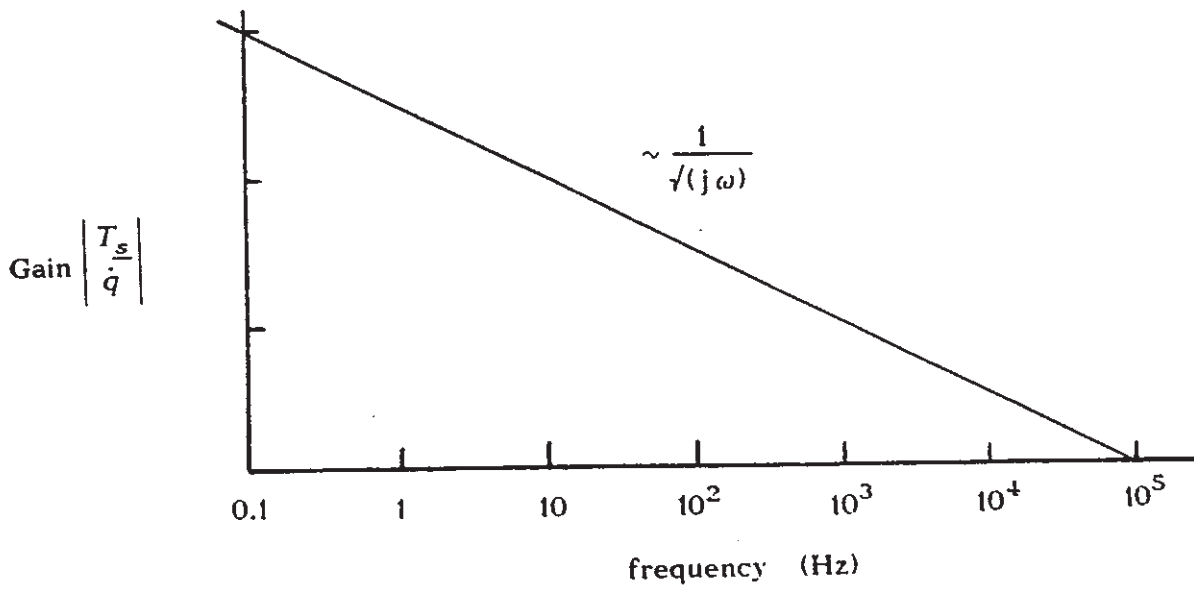
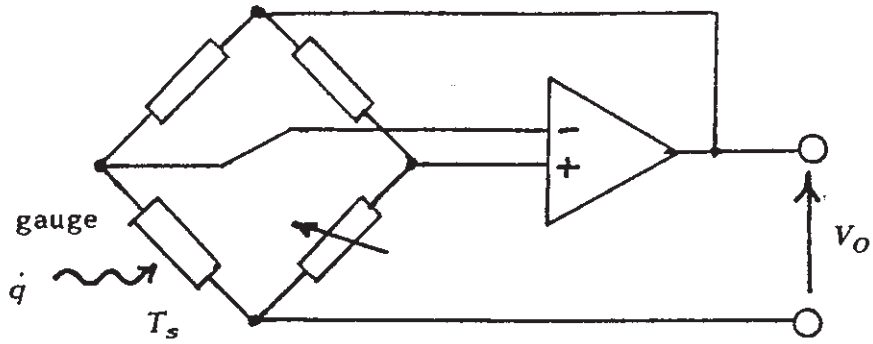


Fig. 9 Variation of thin film gauge response with frequency.





$$\text{Power} \sim V_O^2 \sim \dot{q}_{\text{flow}} + \dot{q}_{\text{substrate}}$$

Fig. 10 Constant temperature circuit for thin film gauges.

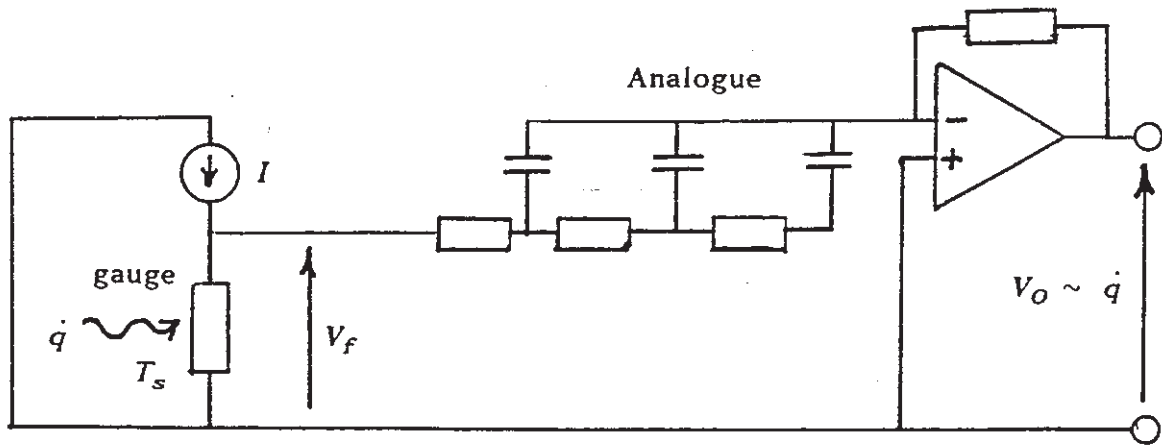


Fig. 11 Constant current circuit for thin film gauges.

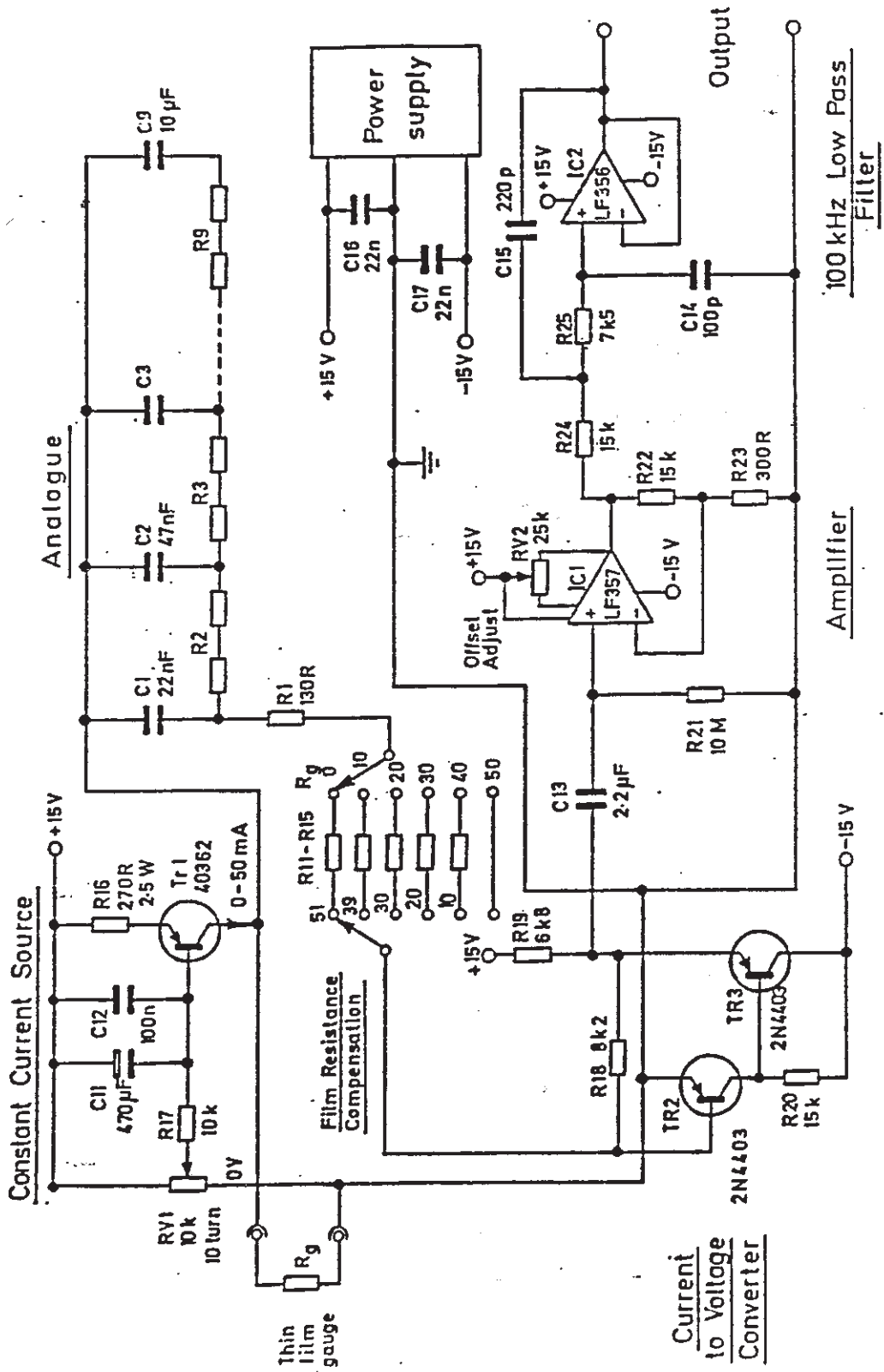


Fig. 12 Practical analogue circuit for use with thin film gauges. From [3].

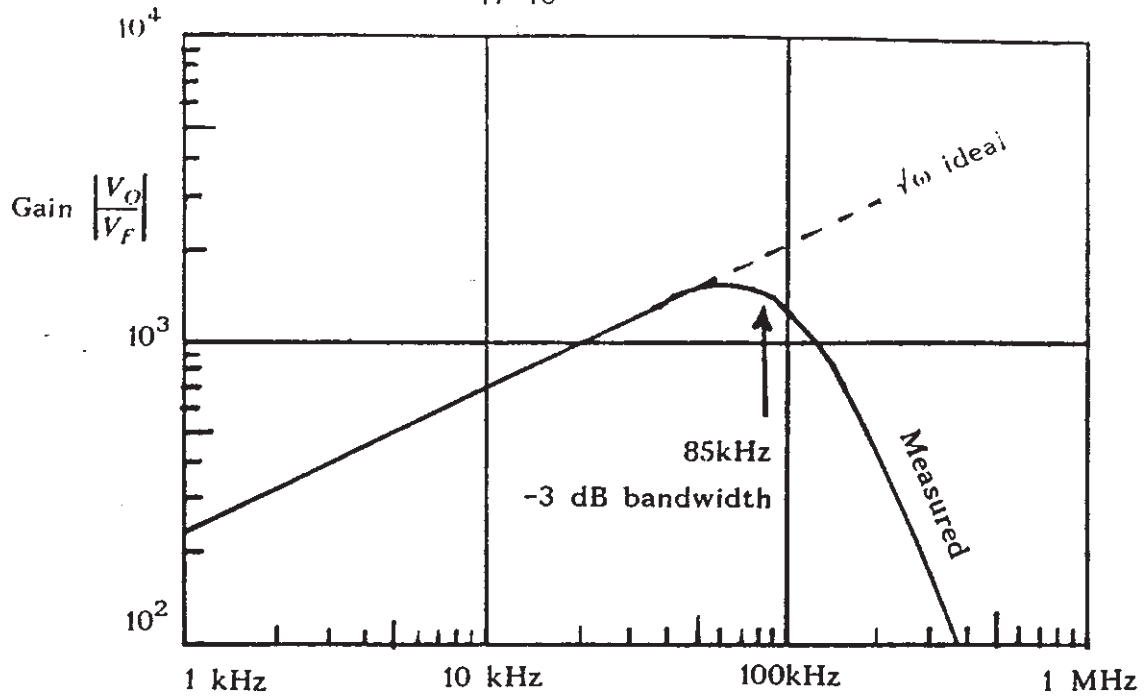


fig. 13 Analogue Gain : frequency response.

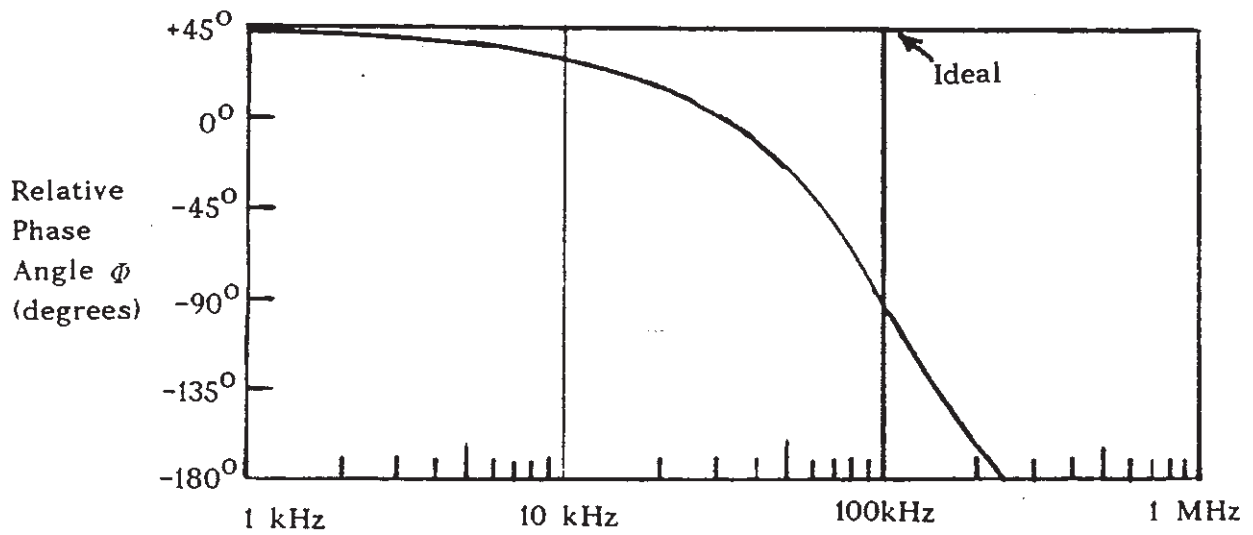


fig. 14 Analogue Phase : frequency response.

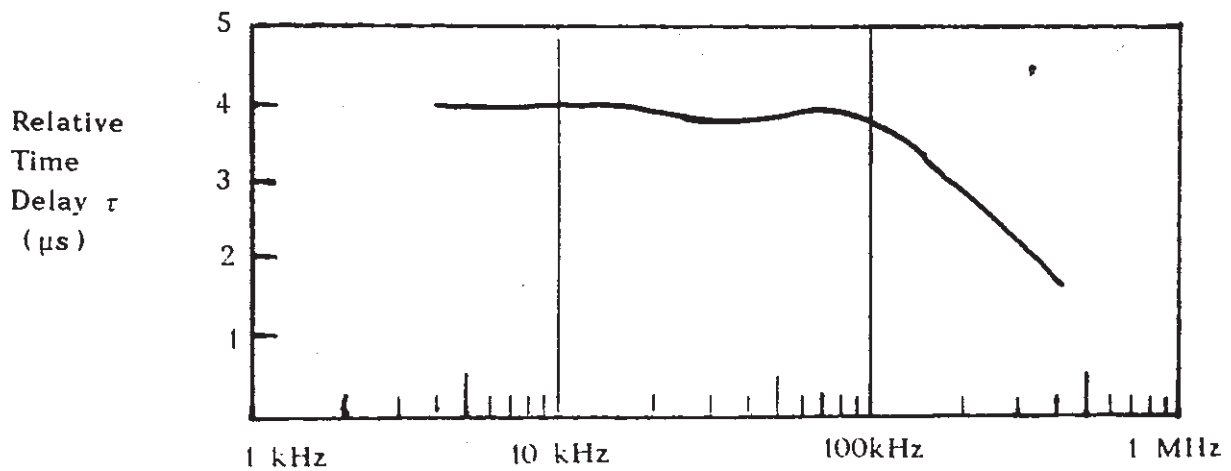


Fig. 15 Analogue Time delay : frequency response.